A Bandpass Filter Using HMSIW-DGS Cell

Y.-M. Huang, Z.-S. He, P.-K. Li, Z.-H. Shao, C.-J. You, and D. Jiang
School of Communication and Information Engineering
University of Electronic Science and Technology of China, Chengdu 611731, China

Abstract— In this paper, a half mode substrate integrated waveguide-to-defected ground structure (HMSIW-DGS) cell, and its embedded structure are proposed to miniaturize a bandpass filter. Both cells can purchase wideband frequency response and low insertion loss, as well as simple and easy fabrication. By cascading two of them according to design requirement, a X-band bandpass filter is designed and measured to meet compact size, low insertion loss, good return loss as well as second harmonic suppression.

1. INTRODUCTION

The half-mode substrate integrated waveguide (HMSIW), derived from substrate integrated waveguide (SIW) with similar high performance and half or so size reduction, has attracted lots of attention due to its merits of easy integration and been widely used in microwave passive components design [1–3]. However, compared with microstrip circuit, the physical size of HMSIW is not small enough, since it just cuts half along the longitudinal direction of SIW, that is to say, its length is still as long as SIW [4].

The defected ground structure (DGS), developed from the photonic bandgap (PBG) structure [5], but much different from the PBG since it needn't to be periodic [6]. As shown in [6], the DGS can change the distribution of the effective permittivity of the substrate, which brings in the change of the distributed capacitance and inductance of the guided wave structure based on this substrate, resulting in the bandgap performance. So the DGS can be used for the circuit size reduction. However, the DGS is etched on the ground plane of the circuit, which makes inconvenience for system integration, since the ground plane of the circuit should be conjunct with the metal shielding cavity. One solution for this drawback is to use the "coplanar DGS", i.e., combining the DGS together with coplanar waveguide (CPW) and SIW [7, 8], which keeps the ground and the transmission line at the same plane. Besides, the complementary split ring resonator (CSRR) [9], loaded on SIW, can be used to realize miniaturized filter since the SIW-CSRR cell can resonate below the cutoff frequency of SIW. However, because of the cascaded coupling scheme of the filters reported in [9], their insertion losses are quite high.

In this paper, a HMSIW-DGS cell, with DGS etched on the top plane of SIW, and its embedded structure, are proposed. And the transmission responses with different parameters are discussed briefly, as well. Based on the proposed cells, a microwave bandpass filter is designed, fabricated and measured. According to the measured results, low insertion loss, good return loss, compact size and suppressed second harmonic are achieved.

2. HMSIW-DGS CELLS

Topologies of proposed HMSIW-DGS cell and its embedded structure are shown in Figures 1(a) and (b), respectively. It can be obtained from the topologies that the cells consist of two parts: the HMSIW section and the DGS section. So it can be expected that the transmission response of the HMSIW-DGS cell contains the inherent highpass characteristic of the HMSIW, which determine the lower sideband cutoff frequency, and the bandgap function of the DGS, which mainly affects the upper stopband, both the cutoff frequency and the rejection strength. As reported in [4], the highpass characteristic of the HMSIW is mainly determined by its width, aw, as shown in Figure 1. And to clarify the property of DGS better, influence of its different geometrical parameters is studied.

Figures 2 and 3 show some full wave simulated results of proposed HMSIW-DGS cell. On one hand, according to Figure 2, as the width of slots' terminal point, $w1$, becomes wider, and the transverse length of slots, $l2$, get longer, the upper sideband bandgap frequency shifts lower, while the lower sideband nearly keeps the same. So it can be predicted that the larger the size of DGS is, the lower the upper sideband bandgap frequency is. On the other hand, as $s1$, the space between two slots, gets wider, the upper sideband bandgap frequency shifts higher heavily, and the central

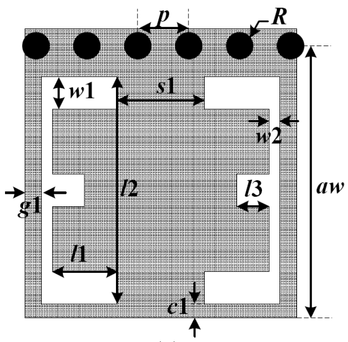

Figure 1: Topologies of (a) HMSIW-DGS cell and (b) embedded form. Black circles, grey zone and white zone represent the metalized via-holes, metal cover and DGS, respectively.

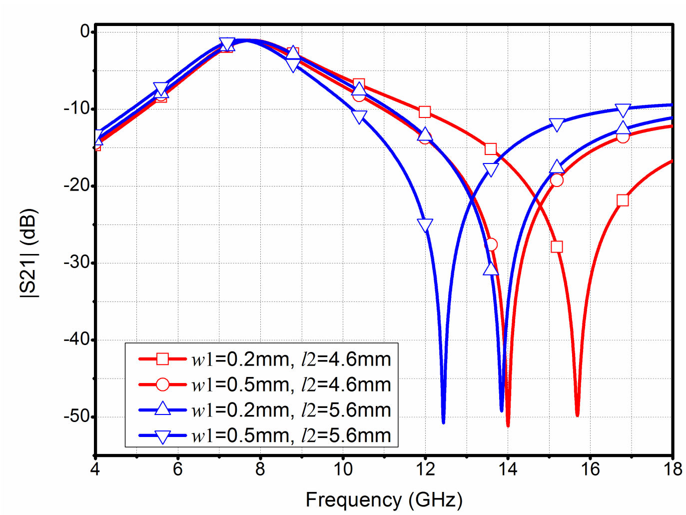

Figure 2: Simulated $|S_{21}|$ of proposed HMSIW-DGS cell with different $l2$ and $w1$. Other geometrical parameters are: $aw = 6\,\text{mm}$, $s1 = 1\,\text{mm}$, $c1 = 0.2\,\text{mm}$, $p = 0.8\,\text{mm}$, $R = 0.2\,\text{mm}$, $g1 = 0.2\,\text{mm}$, $l3 = 0.5\,\text{mm}$, $w2 = 0.2\,\text{mm}$ and $l1 = 1.5\,\text{mm}$.

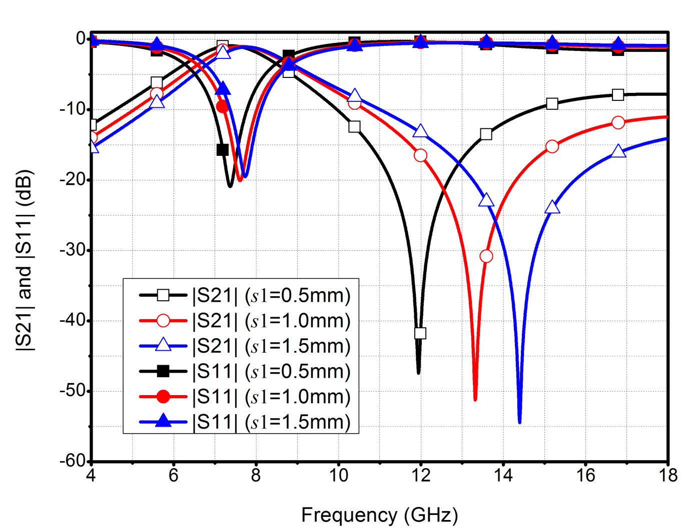

Figure 3: Simulated S-parameters of proposed HMSIW-DGS cell with different $s1$. Other geometrical parameters are: $aw = 6\,\text{mm}$, $c1 = 0.2\,\text{mm}$, $p = 0.8\,\text{mm}$, $R = 0.2\,\text{mm}$, $g1 = 0.2\,\text{mm}$, $l3 = 0.5\,\text{mm}$, $w2 = 0.2\,\text{mm}$, $l1 = 1.5\,\text{mm}$, $w1 = 0.5\,\text{mm}$ and $l2 = 4.6\,\text{mm}$.

operating frequency shifts higher a bit, as shown in Figure 3. All full wave simulation is done based on a substrate with a thickness of 0.254 mm, a relative permittivity of 2.2 and loss tangent of 0.001.

For these phenomena, it can be analyzed by the equivalent circuit model. As discussed in [6], the equivalent circuit model of the DGS can be set as a parallel LC resonator, where L and C represent the distributed inductance and capacitance of DGS, respectively. With this method, it can be obtained easily that: For proposed HMSIW-DGS cell, as $w1$ gets wider or $l2$ gets longer, the distributed inductance increases, so that the bandgap frequency shifts lower; as $s1$ becomes wider, the distributed capacitance decreases, so that the bandgap frequency shifts higher. More accurately, the enlargement of DGS and the broadening of slots' space bring change to both the distributed inductance and capacitance. However, the enlargement of DGS makes the distributed inductance increase more heavily while the broadening of slots' space makes the distributed capacitance decrease more greatly.

3. FILTER DESIGN

Using the proposed HMSIW-DGS cell and its embedded structure as basic unit, a bandpass filter is designed on a RT/Duroid 5880 substrate with a thickness of 0.254 mm, a relative permittivity of 2.2 ± 0.2, and a loss tangent of 0.0009, with its configuration shown in Figure 4. The filter consists of three HMSIW-SIW cells (two single and one embedded form), two half-tapered microstrip-to-SIW transitions and two 50 ohm microstrip transmission lines. Different from the conventional filter design based on resonance and coupling scheme, the filter here is designed by using the transmission scheme. Firstly, the HMSIW-DGS cell and its embedded structure are both operating in transmission form, instead of the resonance form. Secondly, the cascaded combination between

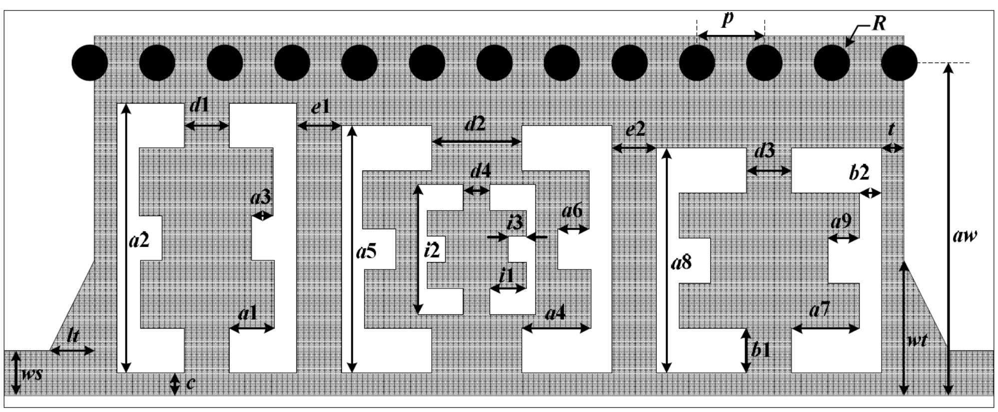

Figure 4: Configuration of the bandpass filter based on proposed HMSIW-DGS cells.

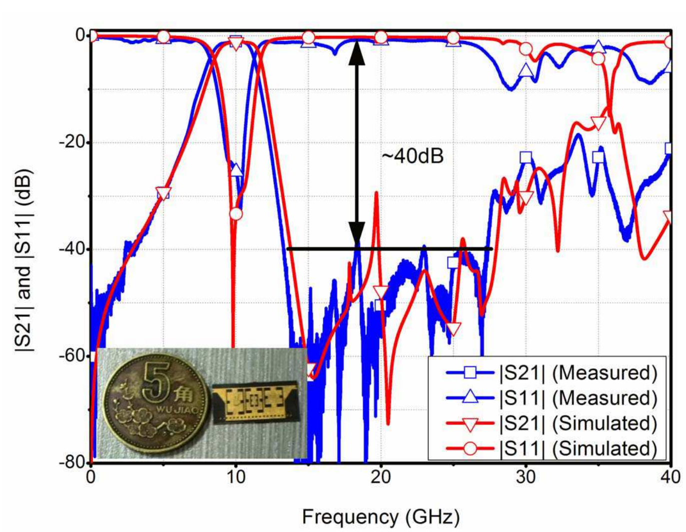

Figure 5: Comparison between measured and simulated results of the proposed HMSIW-DGS filter.

adjacent HMSIW-DGS cells also operates in transmission form. Another pivotal element for the filter design is the external quality factor (Qe). In this filter design, two half-tapered microstrip-to-SIW transitions are used to achieve high Qe, and it can be easily captured that the narrower the tapper width "wt" is, the lower the Qe is. With a wider wt, the Qe is higher, so that the passband insertion loss is lower and the return loss is better. Based on proposed HMSIW-DGS cells with initial parameters operating at the requisite frequency, the filter is tuned and optimized by using a finite element method (FEM) full wave simulator. The optimized dimensions for fabrication are: $aw = 5.5$, $p = 0.8$, $R = 0.2$, $ws = 0.76$, $lt = 1.5$, $wt = 2.5$, $c = 0.2$, $d1 = d2 = d3 = 1$, $e1 = e2 = 0.22$, $t = 0.19$, $a1 = 1$, $a2 = 5.2$, $a3 = 0.5$, $a4 = 1$, $a5 = 5$, $a6 = 0.5$, $a7 = 1.1$, $a8 = 4.1$, $a9 = 0.6$, $i1 = 0.5$, $i2 = 2.4$, $i3 = 0.2$, $d4 = 0.32$, $b1 = 0.6$, $b2 = 0.2$ (unit: mm).

Using a single layer printed circuit board (PCB) process, the filter is fabricated and gold plated. The fabricated filter is measured by an Agilent PNA-X vector network analyzer N5245A. Comparison between measured and simulated results is shown in Figure 5, as well as the photograph of the fabricated filter. It can be obtained from the comparison that the measure results are in good agreement with the simulated ones. The filter is with a central frequency of 10 GHz, a fractional bandwidth of 25%, a return loss is better than 20 dB, and an insertion loss of 1.1 dB, including the loss of two 2.4-mm connectors and only about 0.2 dB higher than the simulated one. Its upper out-of-band rejection is better than 40 dB at the frequency range from 14 GHz to 28 GHz and better than 20 dB up to 40 GHz. That is to say, the filter has quite good second harmonic suppression performance. At last, the overall size of the filter is 15×7 mm, about $0.367\lambda_g^2$, which is quite compact. Table 1 shows some comparisons between proposed filter and some reported filters in references using similar technologies. According to Table 1, compared with filters represented in references, proposed filter is with lower insertion loss, better second harmonic suppression and compacter size. It can also be obtained that the insertion losses of HMSIW structure filters are probably larger than those of SIW structure. The reason for this is that the radiated loss of HMSIW is larger than that of SIW. Since HMSIW is a half closed structure with one radiated side, while SIW is a full closed structure with two column metalized viaholes.

Table 1: Comparison with filters represented in references.

Reference filter	Units number	Topology	f_c (GHz) and FBW*	Insertion loss (dB)	2nd harmonic suppression (dB)	Size (λ_g^2)**
[3]-1	3	HMSIW-slot	7.8 and 22%	1.5	30	0.44
[3]-2	5	HMSIW-slot	8.79 and 40%	1.2	30	0.435
[10]	3	SIW-CSRR	8.15 and 23%	2.16	-	0.77
[11]	3	SIW-CSRR-slot (bottom)	9.4 and 30%	1	30	1.034
Proposed	3	HMSIW-DGS	10 and 25%	1.1	40	0.367

*f_c and FBW stand for central frequency and fractional bandwidth, respectively.
**λ_g stands for the guided wavelength at the central frequency.

4. CONCLUSION

A X-band bandpass filter based on the two proposed HMSIW-DGS cells is designed, fabricated and measured. The measured results show good agreement with the simulated ones. Compared with some reported filters using same technology and operating at similar frequency, the proposed filter has better performance in low insertion loss, compact size and good second harmonic suppression.

ACKNOWLEDGMENT

This work was supported in part by the Excellent Ph.D. Candidate Academic Foundation of UESTC under Grant YBXSZC20131054, the Fundamental Research Funds for the Central Universities under Grant ZYGX2013J006 and the Scientific Research Foundation of UESTC under Grant Y02002010101063.

REFERENCES

1. Hong, W., B. Liu, Y.-Q. Wang, Q.-H. Lai, H.-J. Tang, X.-X Yin, Y.-D. Dong, Y. Zhang, and K. Wu, "Half mode substrate integrated waveguide: A new guided wave structure for mi-

crowave and millimeter wave application," *Proceedings of Joint 31st International Conference on Infrared Millimeter Waves and 14th International Conference on Terahertz Electronics*, 219, Shanghai, China, May 2006.

2. Liu, B., W. Hong, Y.-Q. Wang, Q.-H. Lai, and K. Wu, "Half mode substrate integrated waveguide (HMSIW) 3-dB coupler," *IEEE Microw. Compon. Lett.*, Vol. 54, No. 1, 22–24, 2007.
3. Wang, Y.-Q., W. Hong, Y.-D. Dong, B. Liu, H.-J. Tang, J.-X. Chen, X.-X. Yin, and K. Wu, "Half mode substrate integrated waveguide (HMSIW) bandpass filter," *IEEE Microw. Compon. Lett.*, Vol. 54, No. 4, 265–267, 2007.
4. Lai, Q., C. Fumenaux, W. Hong, and R. Vahldieck, "Characterization of the propagation properties of the half-mode substrate integrated waveguide," *IEEE Trans. Microw. Theory Tech.*, Vol. 57, No. 8, 1996–2004, 2009.
5. Kim, C.-S., J.-S. Park, D. Ahn, and J.-B. Lim, "A novel 1-D periodic defected ground structure for planar circuits," *IEEE Microw. Gui. Wave Lett.*, Vol. 10, No. 4, 131–133, 2000.
6. Ahn, D., J.-S. Park, C.-S. Kim, J. Kim, Y.-X. Qian, and T. Itoh, "A design of the low-pass filter using the novel microstrip defected ground structure," *IEEE Trans. Microw. Theory Tech.*, Vol. 49, 86–93, 2001.
7. Shao, Z.-H. and M. Fujise, "Bandpass filter design based on LTCC and DGS," *Proceedings of Asia-Pacific Microwave Conference*, 138–139, Soochow, China, December 2005.
8. Huang, Y.-M., Z.-H. Shao, and L.-F. Liu, "A substrate integrated waveguide bandpass filter using novel defected ground structure shape," *Progress In Electromagnetics Research*, Vol. 135, 201–213, 2013.
9. Dong, Y.-D., T. Yang, and T. Itoh, "Substrate integrated waveguide loaded by complementary split-ring resonators and its applications to miniaturized waveguide filters," *IEEE Trans. Microw. Theory Tech.*, Vol. 57, 2211–2223, 2009.
10. Deng, K., Z. Guo, C. Li, and W. Che, "A compact planar bandpass filter with wide out-of-band rejection implemented by substrate-integrated waveguide and complementary split-ring resonator," *Microw. Optical Tech. Lett.*, Vol. 53, No. 7, 1483–1487, 2011.
11. Zhang, X.-C., Z.-Y. Yu, and J. Xu, "Novel band-pass substrate integrated waveguide (SIW) filter based on complementary split ring resonators (CSRR)," *Progress In Electromagnetics Research*, Vol. 72, 39–46, 2007.